

The Hamiltonian spectrum of directed percolation

This article has been downloaded from IOPscience. Please scroll down to see the full text article.

1990 J. Phys. A: Math. Gen. 23 3719

(<http://iopscience.iop.org/0305-4470/23/16/020>)

View [the table of contents for this issue](#), or go to the [journal homepage](#) for more

Download details:

IP Address: 129.252.86.83

The article was downloaded on 01/06/2010 at 08:54

Please note that [terms and conditions apply](#).

The Hamiltonian spectrum of directed percolation

Malte Henkel^{†‡} and Hans J Herrmann[‡]

[†] Department of Theoretical Physics, Université de Genève, CH-1211 Genève 4, Switzerland

[‡] Service de Physique Théorique, CEN Saclay, F-91191 Gif-sur-Yvette Cédex, France

Received 28 March 1990

Abstract. We calculate the spectrum of a quantum Hamiltonian which is in the universality class of the Reggeon field theory and directed percolation. We find that its low-lying states follow a self-similarity close to the one encountered in the exactly solvable transverse XY model. The spectrum can, in the finite-size scaling limit, approximately be described by excitations with a dispersion relation k^θ on the lattice instead of the k^2 behaviour of the transverse XY model.

1. Introduction

For models having a conformal invariant critical point many new properties have been discovered in the last few years [1, 2]. Among them it was established that the spectrum of their transfer matrix is composed of regularly spaced ‘towers’ of eigenvalues each coming from a ‘primary’ operator and described by the irreducible representations of the Virasoro algebra. This result which was first predicted theoretically, proved to be an excellent guideline [3] to analyse spectra and find the dimensions of the primary operators.

In directed models the rotational and therefore conformal invariance is broken. Examples are the chiral Potts model [4, 5], directed percolation [6] and various other models [7–10]. Only in special cases, like line defects [11] some results concerning the conformal spectrum-generating algebra similar to those found for rotationally invariant systems can be retrieved. There exist a few results for the form of the correlation functions for dynamical critical phenomena [12] but a more general theory for directed system is still lacking.

The aim of this paper is to investigate the spectra of directed systems. We want to compare the exactly calculable spectrum of a directed Hamiltonian [7] to the low-lying states of directed percolation obtained using numerical techniques. Our hope is to detect common features that could help understanding of the structure of these spectra more generally.

In the following section we will discuss the models and sketch the methods used. In section 3 we present our results for the critical exponents and coupling constants obtained through finite-size scaling. Section 4 is devoted to the discussion and comparison of the spectra and in section 5 we conclude.

2. The models

Directed percolation has been used, for instance, to describe branched structures found in intermittency [13] or to describe the appearance of facets of growing surfaces [14].

Much theoretical work has been done for this model (see, e.g. [6]). It has been shown [15], that it is in the same universality class as the Reggeon field theory (RFT) which made it possible to use results from ε expansions. The d -dimensional RFT has been mapped to a $(d-1)$ -dimensional quantum Hamiltonian [16, 17] which for $d=2$ is:

$$-H = \frac{1}{2} \sum_{j=1}^N (t\sigma_j^z + \sigma_j^x \sigma_{j+1}^x + \sigma_j^y \sigma_{j+1}^y - g\sigma_j^z \sigma_{j+1}^z + ig[(1-\sigma_j^z)\sigma_{j+1}^y + \sigma_j^y(1-\sigma_{j+1}^z)]) \quad (1)$$

with $g=1$, where σ_j are the Pauli matrices on site j and t acts as a temperature. The Hamiltonian H is non-Hermitian, reflecting the directed nature of the model. The correspondence between the RFT and H is given by taking the extreme anisotropic limit $\tau \rightarrow 0$ of the transfer matrix $T = \exp(-\tau h)$ of the RFT. For a recent review on this extreme anisotropic or Hamiltonian limit see [3].

Although H has no obvious global symmetry, there is a 'quasi-symmetry' operator U

$$U = \prod_{j=1}^N \sigma_j^z \quad (2)$$

which takes H into its adjoint $UHU^\dagger = H^\dagger$ which means that the eigenvalues of H are either real or occur in complex conjugate pairs. As we shall see below, at least for the values of t considered here, the imaginary parts of the eigenvalues seem to vanish in the limit $N \rightarrow \infty$. Thus, considering the real parts of the eigenvalues only, it is sensible to speak of the ground state energy and excited states. The ground state energy is given by (if $t \geq 2$)

$$E_0 = -\frac{1}{2}(t-g)N. \quad (3)$$

In the conventional language of directed percolation this translates into the fact that the largest eigenvalue of the transfer matrix is unity [18].

At the critical temperature t_c the gap $\Gamma = E_1 - E_0$ between the ground state E_0 and the first excited state E_1 goes to zero as

$$\xi_{\parallel}^{-1} = \Gamma = |t - t_c|^{\nu_{\parallel}} \quad \xi_{\perp}^{-1} = |t - t_c|^{\nu_{\perp}}. \quad (4)$$

ξ_{\parallel} is the correlation length measured in the single anisotropic direction and ξ_{\perp} is the correlation length in the other $d-1$ directions. In 1+1 dimensions $t_c \sim 2.606$ has been determined using series expansions [19] and the exponents $\nu_{\perp} \sim 1.10$ and $\nu_{\parallel} \sim 1.74$ are known from various methods as seen in table 1.

Table 1. Critical exponents of two-dimensional directed percolation.

ν_{\perp}	θ	Reference
1.101 (3)	1.5807 (10)	this paper
1.0969 (3)	1.5807 (3)	[20]
1.104 (9)	1.572 (1)	[19]
1.094 (1)	1.581 (2)	[18]
1.068 (10)	1.58 (2)	[21]

If one considers the Hamiltonian of (1) on a finite chain of N sites at t_c the correlation length does not grow proportional to N as it does for rotationally invariant systems but fulfils, due to the directedness of the model, a relation [20]

$$\xi_{\parallel} \sim N^{\theta}. \tag{5}$$

The new ‘dynamic’ exponent θ which is often also expressed as $\theta = \nu_{\parallel}/\nu_{\perp}$ or as $\theta = 2/z$ [15, 19] is numerically $\theta \sim 1.58$ in 1+1 dimensions (see table 1).

The case $g=0$ in (1) gives the Hamiltonian of the transverse XY model ($\tau_X Y$) which in 1+1 dimensions can be solved exactly through a Jordan-Wigner transformation [7]. The resulting free fermion theory is

$$H = \sum_{\kappa} \Lambda_{\kappa} (\eta_{\kappa}^{\dagger} \eta_{\kappa} - \frac{1}{2}) \tag{6}$$

where $\Lambda_{\kappa} = |t - 2 \cos \kappa|$ and κ takes the values $\kappa = m\pi/N$ where m is an odd (even) positive integer for the states made out of an even (odd) number of fermionic excitations. At the critical point $t_c(g=0) = 2$, one has a quadratic dispersion relation $\Lambda_{\kappa} \sim \kappa^2$ as opposed to the linear relation found for the conformally invariant Ising model. Various other properties of this model have been calculated analytically [21, 22] and the finite-size scaling at its critical point has been studied [23]. In solid state theory the $\tau_X Y$ model is widely known as the tight-binding model and is used, for example, to describe certain types of metal-insulator transitions [24]. It was also used to describe some regions in the phase diagram of the chiral Potts models [25].

3. Results from finite-size scaling

We have diagonalised the Hamiltonian of (1) for $g = 1$ on finite, closed chains of length N with periodic boundary conditions. Then the translation operator has the eigenvalues $\exp(2\pi i q/N)$, where q corresponds to the discrete momentum and takes the values $0, 1, \dots, N-1 \pmod{N}$. How these momenta are built into the transfer matrix as a phase shift and how the translational symmetry is exploited to reduce the size of the matrix is explained in detail in the literature [3].

The critical temperature and the exponents are extracted from the gaps Γ_N of the finite chains for $q = 0$ using finite-size scaling techniques [20]. In particular we use the relations

$$\frac{\ln[\Gamma_N(t_c)/\Gamma_{N-1}(t_c)]}{\ln[N/(N-1)]} = \frac{\ln[\Gamma_{N+1}(t_c)/\Gamma_N(t_c)]}{\ln[(N+1)/N]} = -\theta \tag{7}$$

to obtain from the first equality, t_c and from the second equality the exponent θ by considering various triplets of system sizes $N-1$, N and $N+1$. Through [20]

$$Z_N = \frac{\ln[(\partial\Gamma_{N+1}/\partial t)/(\partial\Gamma_N/\partial t)]}{\ln[(N+1)/N]} \tag{8}$$

$$\zeta = \frac{1}{2}(Z_{N+1} + Z_N) = \frac{1}{\nu_{\perp}} - \theta \tag{9}$$

we obtain ν_{\perp} where the derivatives are taken at $t = t_{c,N}$ solving (7).

Numerically we solve (7) by calculating, for $q = 0$, the gap Γ_N at various temperatures close to t_c for different chain lengths N and determining the intersections

Table 2. Finite-size values for the critical point, and the critical exponents. ν_{\perp} is obtained by (9). The last line contains the estimates for $N \rightarrow \infty$ as obtained from the BST extrapolation algorithm [28] and the numbers in parentheses give the estimated error in the last digit(s).

sizes	t_c	θ	ζ
2, 3, 4	2.615 75	1.475 80	-0.765 73
3, 4, 5	2.622 61	1.457 10	-0.721 64
4, 5, 6	2.620 43	1.464 44	-0.706 33
5, 6, 7	2.617 73	1.475 42	-0.699 18
6, 7, 8	2.615 53	1.485 89	-0.695 18
7, 8, 9	2.613 84	1.495 08	-0.692 65
8, 9, 10	2.612 55	1.502 98	-0.690 89
9, 10, 11	2.611 55	1.509 74	-0.689 58
10, 11, 12	2.610 78	1.515 56	-0.688 54
11, 12, 13	2.610 16	1.520 59	-0.687 69
12, 13, 14	2.609 66	1.524 97	-0.686 96
13, 14, 15	2.609 25	1.528 81	-0.686 33
14, 15, 16	2.608 92	1.532 19	-0.685 77
∞	2.606 40 (7)	1.5807 (10)	-0.6728 (25)

of the curves using interpolation techniques. In table 2, we give the finite-size data obtained for t_c , θ and ζ . The extrapolation towards the $N \rightarrow \infty$ limit was done using the BST extrapolation algorithm described in [26]. Detailed reviews on extrapolation techniques are given in [27, 28]. We find for the critical point

$$t_c = 2.606\,40 \pm 0.000\,07 \quad (10)$$

which is in good agreement with that $t_c = 2.606\,28(4)$ found previously [19] from series expansions. For the exponents we obtain:

$$\theta = 1.5807\,(10) \quad \text{and} \quad \nu_{\perp} = 1.101\,(3). \quad (11)$$

The effective correction-to-scaling exponent is $\omega = 1.1 \pm 0.1$. As can be seen from table 1 our value for θ is in excellent agreement with the most accurate determination so far [29]; for ν_{\perp} our error bars are unfortunately rather large. Since we used a different method than in [19] the agreement of our exponents with that of directed percolation reconfirms that the quantum Hamiltonian of (1) and directed percolation are in the same universality class.

4. Discussion of the spectrum

Before describing our results for the spectrum, let us first consider the convergence of the finite-size data. We are interested in the amplitudes A_i of the energy gaps $\Gamma_i = E_i - E_0$

$$A_i = N^{\theta} \Gamma_i. \quad (12)$$

In figure 1, we give as an example the data for the case $q = 0$. We note that an extrapolation in $1/N$ works rather well. However, in spite of the relatively large lattices with up to seventeen sites available, we see that the finite-size data $A_{i,N}$ themselves are still quite far from their values in the $n \rightarrow \infty$ limit, so that some extrapolation is always necessary. Since our values for E_i are very precise (a variation of t_c within its error bars only affords the fourth decimal place of the E_i), it is also possible to use

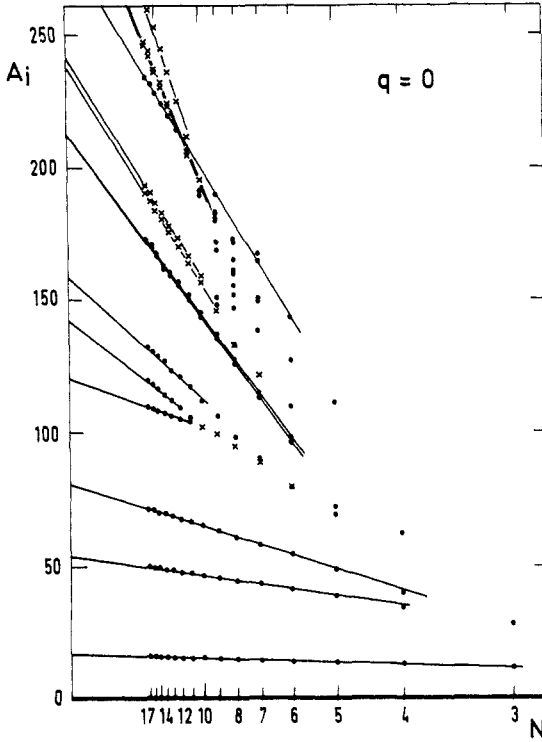


Figure 1. Amplitude spectrum $A_i(N)$ of the quantum Hamiltonian of (1) for $g = 1$ and $q = 0$ for a finite chain of length N plotted against N^{-1} . The intercept gives the spectrum in the thermodynamic limit. For complex conjugate pairs (crosses) we show the real part, while real eigenvalues are shown as dots.

more sophisticated extrapolation techniques, like the ratio method, the BST algorithm or others [27, 28]. Similar plots were obtained for the case $q \neq 0$ where lattices up to $N = 15$ were used. Note that when calculating the A_i from (12), the amplitude spectrum does depend on the estimated value of the exponent θ . We have also tried to obtain the A_i directly, without having to know θ , from the relation

$$\frac{\ln \Gamma_i(N+1)}{\ln(N+1)} - \frac{\ln \Gamma_i(N)}{\ln N} = \ln A_i \left(\frac{1}{\ln(N+1)} - \frac{1}{\ln N} \right) \tag{13}$$

but the finite-size estimates obtained this way show no clear convergence with N .

As can be seen from figure 1 some of the levels split up into two levels after a certain size is reached. This is because for small sizes these eigenvalues are in fact a pair of complex conjugate numbers of which we just plot the real part. In some cases we even find complex conjugate pairs for the largest systems considered. We believe that these levels might be just nearly degenerate and that the split-up will occur at sizes much larger than we can treat numerically or that the imaginary parts vanish when $N \rightarrow \infty$ leaving a doubly degenerate real-valued energy level.

In figure 2(a) we show the resulting extrapolated spectrum for various values of q . The numerical accuracy strongly decreases with increasing energy so that the highest energy levels in figure 2(a) have an uncertainty of about 20%. Some levels are shown

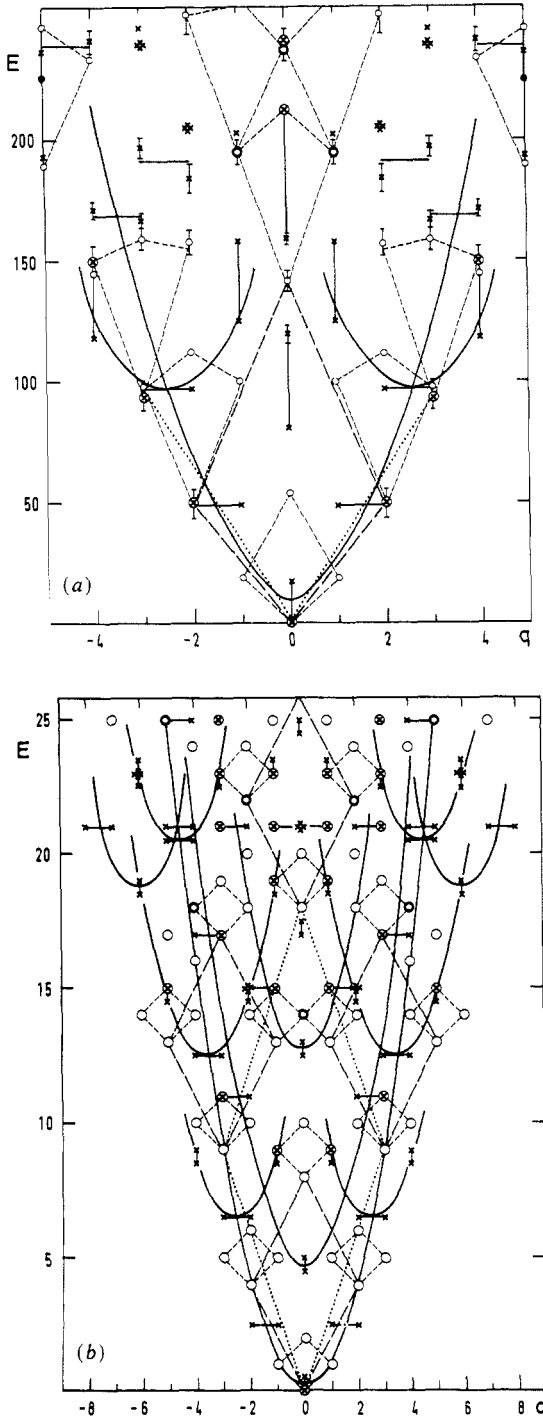


Figure 2. Low-lying part of the amplitude spectrum A_i at t_c for different momenta q of (a) the quantum Hamiltonian of directed percolation, i.e. $g = 1$ in (1), and (b) the transverse XY model, i.e. $g = 0$ in (1). The crosses (circles) are even (odd) eigenvalues and the full (broken) lines are guides to the eye to visualise the self-similarity of the even (odd) sector.

as doubly degenerate, these are complex conjugate pairs for which only the real part is shown.

We oppose our spectrum to the exactly calculable spectrum of the $\tau\chi\chi$ model at its critical point $t_c = 2$ shown in figure 2(b). The spectrum is obtained by the superposition of the one-particle excitations of (6) with discrete one-particle momenta $k = m/2$ and the sum of the k 's will give the total discrete momentum q . Since the $\tau\chi\chi$ model has a global spin-flip symmetry the spectrum decomposes in an even sector (crosses) and an odd sector (circles). We see that the spectrum of each sector has a self-similar structure.

The odd sector is made out of small rhombi that come from excitations (particles) of momentum $+1$ and/or -1 of a given level. These rhombi are placed within larger rhombi stemming from particles of momenta ± 2 which themselves lie in larger rhombi coming from ± 3 momenta particles and so on. We show the first generations of this hierarchical structure by broken lines in figure 2(b).

The even sector consists of two types of pairs, the horizontal and the vertical ones that are due to $\pm \frac{1}{2}$ excitations. These pairs lie on parabolas of the form $(k + \frac{1}{2})^2 + (\frac{1}{2})^2$ having their minimas at energies $(k' + \frac{1}{2})^2$ where k and k' are positive integers and k' is odd. On each parabola each level k is itself the starting point of a parabola of $(k - 1)$ levels. These secondary parabolas themselves have side-branching parabolas and a hierarchical tree-like structure of parabolas is obtained. This self-similar structure can also be explained by the superposition of non-interacting particles with a quadratic dispersion relation which is not surprising in view of (6). At higher energies one obtains in addition other complex self-similar structures due to more complicated combinations of particles but we only want to focus here on the low-lying levels.

Considering now again the spectrum of directed percolation we see in figure 2(a) that simply by analogy with the spectrum of figure 2(b) it is possible to identify 'even' and 'odd' sectors. This is surprising since there is no apparent global symmetry in directed percolation. Continuing the comparison of the two spectra one can also recognise in figure 2(a) remnants of the self-similarity that we discussed for the spectrum of the $\tau\chi\chi$ model. The rhombi in the 'odd' sector are no longer equilateral which can be interpreted in the particle picture of the $\tau\chi\chi$ model by an interaction between the particles: two excitations can either from a bonding or an anti-bonding state giving rise either to a shorter or to a longer upper part of the rhombi. Note that the 'small' and 'larger' rhombi are still similar to each other. We also see the hierarchical tree-like structure of 'parabolas' in the 'even' sector. The horizontal pairs stemming from $+\frac{1}{2}$ excitations are, however, no longer of equal length: $A + \frac{1}{2}$ excitation costs more energy if added to a higher level and this energy seems numerically proportional to the quantum number k' of the level.

In figure 2(a) the external 'parabola' is given by values 0.82, 5.0, 9.7 and 16.6 which can be fitted by $(k + \frac{1}{2})^\theta + (\frac{1}{2})^\theta$ giving the sequence 0.7, 4.7, 9.7 and 16.0, while if one tries a fit of the form $(k + \frac{1}{2})^2 + (\frac{1}{2})^2$ one gets at best 0.37, 3.7, 9.7 and 18.3. Similarly the minima of the 'parabolas' can be fitted better by k'^θ than by k'^2 (k' odd) and the same applies also to the sequence of starting points of new generations of rhombi. So it seems that one can rather well quantitatively reproduce some of the low-lying states of the spectrum if one replaces the quadratic dependence on k that one has in the $\tau\chi\chi$ model by a k^θ dependence, in spite of the fact that the $g = 1$ model is not a free-particle theory.

Note that this k^θ law was obtained taking the limit $N \rightarrow \infty$ and k fixed. The continuum dispersion relation $E(P)$, however, is obtained by the limit $N \rightarrow \infty$, $q \rightarrow 0$

and $P = 2\pi q/N$ fixed. We have tried for a relation $E \sim P^\alpha$ (in a Brillouin zone) but the still relatively few lattices do not really permit to distinguish between $\alpha = 2$ and $\alpha = \theta$, although the available data favour $\alpha = 2$ in the region $0.3 \leq q/N \leq 0.5$.

Finally, let us make a comment on the ground state energy. From (3) we see that E_0 only contains a (non-universal) bulk term bN and that in particular the universal finite-size scaling amplitude f in $e_0 \approx bN + fN^{-x}$ vanishes for both $g = 0$ with $x = 2$ and $g = 1$ with $x = \theta$. (The bulk term bN could obviously be made to vanish by a simple redefinition of the diagonal part of the Hamiltonian (1).) In this context it is perhaps also worth recalling that the ground state energy of the effective Hamiltonian describing model A of critical dynamics vanishes similarly [30]. This finding should be compared with conformally invariant systems, where the corresponding universal amplitude is related to the central charge of the spectrum-generating Virasoro algebra [2]. Further studies on directed systems will hopefully explain this observation.

5. Conclusion

We have analysed for the first time the spectra of directed problems. For the two models that we studied, i.e. directed percolation and the transverse XY model we found that the low-lying part of the spectrum has a self-similar structure in energy-momentum space. The spectrum of the exactly solvable τ XY model follows in the finite-size scaling limit a dispersion relation k^2 and the numerical evidence for directed percolation supports a relation k^θ . By analogy with the picture of elementary excitations (particles) that build up the spectrum of the τ XY model we propose that the spectrum of directed percolation is the result of interacting particles. We hope that future theoretical work on directed models might lead to an explanation of our proposed picture. For this purpose also further empirical evidence from other directed models would be useful.

As a by-product of our numerical work we obtained new estimates for the critical exponents and the location of the critical point and reconfirmed that the Hamiltonian formulation of the Reggeon field theory is in the same universality class as directed percolation.

Acknowledgment

One of us (MH) thanks the Wissenschaftsausschuss of Nato via DAAD for financial support.

References

- [1] Cardy J L 1987 *Phase Transitions and Critical Phenomena* vol 11, ed C Domb and J Lebowitz (New York: Academic) p 55
- [2] Cardy J L 1990 *Fields, Strings and Critical Phenomena (Les Houches XLIX)* ed E Brézin and J Zinn-Justin (Amsterdam: North-Holland) p 169
- [3] Henkel M 1990 *Finite-size Scaling and Numerical Simulation of Statistical Systems* ed V Privman (Singapore: World Scientific) p 353
- [4] Baxter R J 1989 *J. Stat. Phys.* **57** 1
- [5] Albertini G, McCoy B M and Perk J H H 1989 *Phys. Lett.* **135A** 159; 1989 *Phys. Lett.* **139A** 204

- [6] Kinzel W 1983 *Percolation Structures and Processes* ed G Deutscher, R Zallen and J Adler (Bristol: Hilger) p 425
- [7] Katsura S 1962 *Phys. Rev.* **127** 1508
- [8] Nadal J P, Derrida B and Vannimenus J 1982 *J. Physique* **43** 1561
- [9] Vescan T, von Gehlen G and Rittenberg V 1986 *J. Phys. A: Math. Gen.* **19** 1957
- [10] Everts H U and Röder H 1989 *J. Phys. A: Math. Gen.* **22** 2475
- [11] Henkel M, Patkós A and Schlottmann M 1989 *Nucl. Phys. B* **314** 609
- [12] Cardy J L 1985 *J. Phys. A: Math. Gen.* **18** 2771
- [13] Chaté H and Manneville P 1988 *Phys. Rev. A* **38** 4351
- [14] Richardson D 1973 *Proc. Camb. Phil. Soc.* **74** 515
Savit R and Ziff R 1985 *Phys. Rev. Lett.* **55** 2515
- [15] Cardy J L and Sugar R L 1980 *J. Phys. A: Math. Gen.* **13** L423
- [16] Brower R C, Furman M A and Subbarao K 1977 *Phys. Rev. D* **15** 1756
- [17] Amati D, Ciafaloni M, Le Bellac M and Marchesini G 1976 *Nucl. Phys. B* **112** 107
- [18] Kinzel W and Yeomans J M 1981 *J. Phys. A: Math. Gen.* **14** L163
- [19] Brower R C, Furman M A and Moshe M 1978 *Phys. Lett.* **76B** 213
- [20] Essam J W, Guttmann A J and De'Bell K 1988 *J. Phys. A: Math. Gen.* **21** 3815
- [21] Grassberger P and de la Torre A 1979 *Ann. Phys.* **122** 373
- [22] Domany E and Schaub B 1984 *Phys. Rev. B* **29** 4095
- [23] Niemeyer T 1967 *Physica* **36** 377
- [24] Barouch E and McCoy B M 1971 *Phys. Rev. A* **3** 786
- [25] Hoeger C, von Gehlen G and Rittenberg V 1985 *J. Phys. A: Math. Gen.* **18** 1813
- [26] den Nijs M 1988 *Phase Transitions and Critical Phenomena* vol 12, ed C Domb and J Lebowitz (New York: Academic) p 220
- [27] Howes S, Kadanoff L P and den Nijs M 1983 *Nucl. Phys. B* **215** 169
- [28] Henkel M and Schütz G 1988 *J. Phys. A: Math. Gen.* **21** 2617
- [29] Guttmann A J 1989 *Phase Transitions and Critical Phenomena* vol 13, ed C Domb and J Lebowitz (New York: Academic) p 1
- [30] Weniger E J 1989 *Comp. Phys. Rep.* **10** 189
- [31] Goldschmidt Y Y 1987 *Nucl. Phys. B* **280** 340
Niel J C and Zinn-Justin J 1987 *Nucl. Phys. B* **280** 355